Gait Analysis by Causal Decomposition

Xiaohang Peng, Yukun Feng, Shengjie Ji, Joan Toluwani Amos, Wenan Wang, Min Li, Shaolong Ai,
Xiangzhe Qiu, Yeyun Dong, Dan Ma, Dezhong Yao, *Senior Member, IEEE,*
Pedro A. Valdes-Sosa, and Peng Ren

Abstract—**Recent studies have investigated bilateral gaits based on the causality analysis of kinetic (or kinematic) signals recorded using both feet. However, these approaches have not considered the influence of their simultaneous causation, which might lead to inaccurate causality inference. Furthermore, the causal interaction of these signals has not been investigated within their frequency domain. Therefore, in this study we attempted to employ a causal-decomposition approach to analyze bilateral gait. The vertical ground reaction force (VGRF) signals of Parkinson's disease (PD) patients and healthy control (HC) individuals were taken as an example to illustrate this method. To achieve this, we used ensemble empirical mode decomposition to decompose the left and right VGRF signals into intrinsic mode functions (IMFs) from the high to low frequency bands. The causal interaction strength (CIS) between each pair of IMFs was then assessed through the use of their instantaneous phase dependency. The results show that the CISes between pairwise IMFs decomposed in the high frequency band of VGRF signals can not only markedly distinguish PD patients from HC individuals, but also found a significant correlation with disease progression, while other pairwise IMFs were not able to produce this. In sum, we found for the first time that the frequency specific causality of bilateral gait may reflect the health status and disease progression of individuals. This finding may help to understand the underlying mechanisms of walking and walking-related diseases, and offer broad applications in the fields of medicine and engineering.**

Index Terms—**Causal decomposition, ensemble empirical mode decomposition (EEMD), frequency domain, gait analysis, Hilbert transform, instantaneous phase, Parkinson's disease (PD), phase coherence.**

I. Introduction

A. Walking Mechanisms and Quantitative Gait Analysis

WALKING is one of the most important movements in a person's daily life, and mainly involves the locomotion of the human body through the coordination of both legs. Although walking seems to be quite simple, it actually involves the participation of a number of different physiological components, including the muscles, joints, cerebral cortex, cerebellum, spinal cord, and more. It should be noted that if there is a problem in any one of these physiological components, it may produce an abnormal gait in the individual. Therefore, quantitative analysis of individual gait patterns has become an important way to understand the mechanisms of walking and diseases related to it.

Quantitative gait analysis usually involves the study of an individual's walking patterns through the collection and analysis of the person's physiological, kinetic, and kinematic signals, such as their electromyographic signals, vertical ground reaction force (VGRF), and acceleration signals, and these have been broadly applied in many different fields to date. For example, many different diseases are related to abnormal gait, including cerebral palsy, Parkinson's disease (PD), Huntington's disease, and stroke. Quantitative gait analysis based on kinetic (or kinematic) signals not only helps clinicians to diagnose these diseases, but can also be used as a standard tool to evaluate the rehabilitative effect of their treatment. In addition, performing quantitative analysis on the gait patterns of children and the elderly can help the clinicians to assess their physical development and aging process. Furthermore, many wearable devices on the market can be used to monitor personal health by collecting and analyzing real-time walking data such as gait rhythm. It can thus be seen that quantitative gait analysis plays an increasingly important role in the fields of medicine and engineering.

B. Performing Bilateral Gait Analysis Through Causal Decomposition

There have been many previous studies on quantitative gait analysis. For example, Joshi *et al.* extracted gait parameters based on performing wavelet decomposition of time series of stride time intervals, swing time intervals, and stance time intervals, and successfully differentiated PD patients from healthy control (HC) individuals [1]. Anna *et al.* proposed a symbol-based approach for acceleration signals, and this was regarded as a new measure to evaluate walking symmetry [2]. Gouwanda *et al.* used normalized cross-correlation to evaluate

the waveform patterns generated by the lower limb in each gait cycle, and found that normalized cross-correlation can be considered as a single value indicator that determines the gait asymmetry [3]. Although all of these previous studies quantified gait patterns from different perspectives, they did not investigate how both left and right legs causally influence each other while walking, i.e., they did not explore the causality of bilateral gait, not until a recent paper published by Gong *et al.* [4]. In that study, a causality index was calculated based on the acceleration signals recorded from bilateral knee joints in order to differentiate individuals with multiple sclerosis from HC. However, this study still contained a number of insufficiencies: (1) The calculated causality index is mainly based on the concept of Bayesian prediction; that is, the events occurring in the past contribute to predicting the current state (the effect). A time lag between cause and effect is thus required for causal reasoning. However, cause and effect may also be able to influence each other simultaneously, and this phenomenon is widely present in the physiological regulation of body functions [5], [6]. In other words, at the moment when an effect manifests, it is always affected by both current and past causes. More importantly, recent studies have already indicated that a cause-effect relationship cannot be accurately inferred without considering their simultaneous influence [5]–[7]. Therefore, it can be seen that the methods employed in [4] may not only underestimate the simultaneous nature of the cause-effect relationship observed in bilateral gait, but also lead to inaccurate causal inference. (2) The time domain information of acceleration signals employed in [4] might not be enough to capture the causal interaction between both legs during walking, since human gait is a periodic, rhythmic, and dynamic process of movement [8]. Furthermore, the oscillatory components for kinetic and kinematic signals within specific frequency bands generally have different physiological meanings [9], [10]. Thus, it is very reasonable to investigate the frequency-specific causal interaction of kinetic (or kinematic) signals in both left and right feet. Due to the reasons mentioned above, in this study we tried to analyze bilateral gait through causal decomposition.

It is worth noting that the method of causal decomposition is not based on the time dependency of the two signals, but on the instantaneous phase dependency between their oscillatory components in a specific frequency band. Furthermore, we define the cause-effect relationship of the two signals (e. g. A and B) according to the principle of covariation of cause and effect [11]. Specifically, when a component in B that is causally related to A is removed from B, if the instantaneous phase dependency between these two signals is diminished, then we can assert that B causes A, but not vice versa [12]. In addition, this approach also considers simultaneous cause and effect relationships not accounted for by predictive causality methods used in [4].

Abnormal gait is one of the main symptoms of many diseases, and it is almost impossible to list them exhaustively in this article. Therefore, in this study, we only chose to analyze PD patients, which may be regarded as a sample to illustrate this method. In addition, the VGRF signals of PD patients have been widely analyzed in order to characterize their walking patterns, which are known as one of the most important kinetic signals for gait analysis. However, there is no current research which has used VGRF to quantify the mutual causal influence between the legs during walking. Apart from this, some previous studies have shown that different frequency components of VGRF signals can generally reflect a diverse set of walking mechanisms [9], [10]. Therefore, this study attempts to employ the method of causal decomposition to analyze the bilateral VGRF signals of HC individuals and PD patients in order to reveal whether the disease changes the causality of specific frequency components while they walk.

II. Materials and Methods

A. Data Records and Preprocessing

The data set used in this study was collected by Hausdorff *et al.*, and can be obtained from PhysioNet [13]. This data set includes 93 PD patients (age: 66.3 ± 9.5 (SD) years; 58 males and 35 females) and 73 HC subjects (age: 63.7 ± 8.7 (SD) years, 40 males and 33 females). During the experiment, all subjects were required to walk at a self-selected pace for approximately 2 minutes on level ground. Eight sensors (Ultraflex Computer Dyno Graphy, Infotronic Inc.) were applied underneath each foot in order to record the VGRF signals of individuals during the walking process. All VGRF signals were digitized and sampled at 100 Hz. Apart from this, the total VGRF signal of each foot is provided in this data set as well, and is composed as the sum total of the 8 sensors' outputs. It should be noted that the total VGRF signals were used for analysis in this study, and in the following text all references to "VGRF signals" refer to total force signals. Finally, this data set also contains the clinical scale scores of each PD patient, including their Hoehn & Yahr (HY) scale score (a commonly used clinical scale for evaluating the progression of PD) and the individual's time up and go (TUG) test score (a commonly used screening tool to assist clinicians to identify patients at risk of falling).

In data preprocessing portion, a fourth order Butterworth low-pass filter with a 25Hz cutoff frequency was employed, and this has been proved to be able to eliminate 99% of noise while retaining all major components of the VGRF signal [14].

B. Causal Decomposition

In this study, the causal decomposition method was used to detect the causal relationship between pairwise IMFs extracted from the VGRF signals of both left and right feet. Here, causality inference is based the covariation principle proposed by Galilei: cause is that which, once present, is followed after by effect; if removed, the effect is then removed [11]. To achieve this, three steps are required: (1) using the EEMD to decompose each VGRF signal into a finite number of sub-band components, namely IMFs (the numbers of decomposed IMFs are the same for both VGRF signals); (2) calculating the instantaneous phase of each IMF via Hilbert transform; (3) estimating the causal interaction strength (CIS) between paired IMFs [12].

1) Ensemble Empirical Mode Decomposition: In this paper, the method of EEMD was adopted to decompose the preprocessed VGRF signal into a finite number of components with different frequency distributions, namely IMFs. EEMD has many advantages, such as being data-driven, locally adaptive, multi-scale, and robust [15]. Furthermore, it is also

very suitable for processing non-stationary, non-linear, and time-varying data [15]. Thus, in this study the EEMD was selected to decompose VGRF signals first, and its procedures contain three parts, which are shown as follows:

Step 1: In the preprocessed VGRF signal, random white noise weighted by coefficients is added to form a set of noise-added signals, which can be expressed as follows:

$$S_k(t) = S(t) + r \times w_k(t) \quad (k = 1, \dots, K) \tag{1}$$

where $S(t)$ is a preprocessed VGRF signal and w_k is the kth added white noise weighted by amplitude coefficient r. $S_k(t)$ is the kth noise-added signal. K is the number of signals added with different white noise, namely the number of ensemble members.

Step 2: Decompose each noise-added signal into IMFs.

(a). Take $S_k(t)$ as the initial signal. Identify and record its local maxima and minima.

(b). Construct the cubic spline curve between each two adjacent maxima to form upper envelope, denoted as $E_u(t)$.

(c). Construct the cubic spline curve between each two adjacent minima to form the lower envelope, denoted as $E_l(t)$.

(d). Take the average of $E_u(t)$ and $E_l(t)$ to obtain its averaged envelope $m_{k1}(t)$:

$$m_{k1}(t) = \frac{1}{2}(E_u(t) + E_l(t)) \quad (k = 1, \dots, K) \tag{2}$$

(e). Make the difference between $S_k(t)$ and $m_{k1}(t)$:

$$S_{k1}(t) = S_k(t) - m_{k1}(t) \quad (k = 1, \dots, K) \tag{3}$$

where $S_{k1}(t)$ denotes the first IMF decomposed from the preprocessed VGRF signal added with kth white noise.

(f). Set first residue res_{k1} equal to $m_{k1}(t)$. Thus, the following equation can be obtained:

$$res_{k1} = S_k(t) - S_{k1}(t) \quad (k = 1, \dots, K) \tag{4}$$

(g). Iterate steps (a)-(f) on the $res_{k(j-1)}$, which is generated in the latest iteration, and the following IMFs can be obtained as follows:

$$res_{k(j-1)} - res_{kj} = S_{kj}(k = 1, \dots, K; j = 2, 3 \dots, J) \tag{5}$$

where S_{kj} represents the jth IMF of the preprocessed VGRF signal added by the kth white noise, and res_{kj} indicates the residual generated in the jth iteration. J represents the maximum number of IMFs decomposed from the preprocessed VGRF signal added by the kth white noise.

Such iterations will stop only when res_{kj} is smaller than the predefined threshold, or the number of IMFs reaches a certain limit [12]. The kth noise-added signal can then be expressed as:

$$S_k(t) = \sum_{j=1}^{J} S_{kj} + res_{kJ} \quad (k = 1, \dots, K; j = 1, \dots, J) \tag{6}$$

where res_{kJ} denotes the residual generated in the last iteration of the decomposition of $S_k(t)$.

Step 3: For each white noise added signal $S_k(t)$, its decomposed IMFs, $S_{kj}(t)$ $(j = 1, 2, \dots)$, can be obtained from step 1 and 2. Then, because of the zero-mean nature of white noise, the different white noise attached to each decomposed IMF S_{kj}

can be cancelled out by summing, and the final IMFs S_j can be obtained by

$$S_j = \frac{1}{K} \sum_{k=1}^{K} S_{kj} \quad (j = 1, \dots, J) \tag{7}$$

Thus, the original signal can be expressed as follows:

$$S(t) = \sum_{j=1}^{J} S_j(t) + res_J \tag{8}$$

where res_J is the average of $res_{kJ}(k = 1, \dots, K)$. In this study, we attempted to decompose a VGRF signal into three IMFs to represent high, intermediate, and low-frequency components. J is thus designated as 3. Figure 1 shows the EEMD analysis of VGRF signals obtained from one HC individual and one PD patient, where the S^L and S^R represent the VGRF signal extracted from left foot and right foot respectively.

It is worth noting that there are two parameters which must be specified in advance in practice of EEMD, namely the number of ensemble members K and noise amplitude r, both of which play an important role in EEMD calculation. Theoretically, using the statistical characteristics of white noise, i.e. zero mean, we can obtain the true IMFs since a collection of white noise cancels each other out during the averaging process, as can be seen in (7). But in fact, if K is not large enough, the added noise would not be completely canceled out, producing biased IMFs [15]. With regard to parameter r, as illustrated in (1), the added noise will become a fraction of the decomposed signal. If r is too large, the original signal will be covered. On the contrary, if r is too small, it would not be an effective tool to simulate the different levels of noise present in the process of signal collection [15]. Apart from this, in order to better reconstruct the original signal, its decomposed IMFs should remain orthogonal or nearly orthogonal to each other. However, the additional noise will interfere with the manifestation of the original signal, thereby affecting the orthogonality of the IMFs [16]. It can thus be seen that the value selections for r and K are very important for EEMD analysis. For more details about parameter selection, please refer to the supplementary material.

2) Hilbert Transform: The Hilbert transform is the second part of causal decomposition. Specifically, the Hilbert transform of decomposed IMFs, namely S_j, is defined as $S_{jH} = \frac{1}{\pi} \int \frac{S_j(\tau)}{t-\tau} d\tau$, thereby its instantaneous amplitude is defined as $A_j(t) = \sqrt{S_j^2(t) + S_{jH}^2(t)}$, and the instantaneous phase is defined as $\varphi_j(t) = \arctan(\frac{S_{jH}(t)}{S_j(t)})$ [12]. With this transform, each IMF can be represented by instantaneous amplitude and instantaneous phase, which is shown as follows:

$$S_j(t) = A_j(t) \cos \varphi_j(t) \quad (j = 1, \dots, J) \tag{9}$$

3) Causality Estimation:

a) Phase Coherence: Two nonlinear coupled oscillators may synchronize their phase, even if their amplitudes remain uncorrelated [17]. This phenomenon is known as phase synchronization, and can be measured using several indexes, such as phase coherence. In this study, phase coherence between the
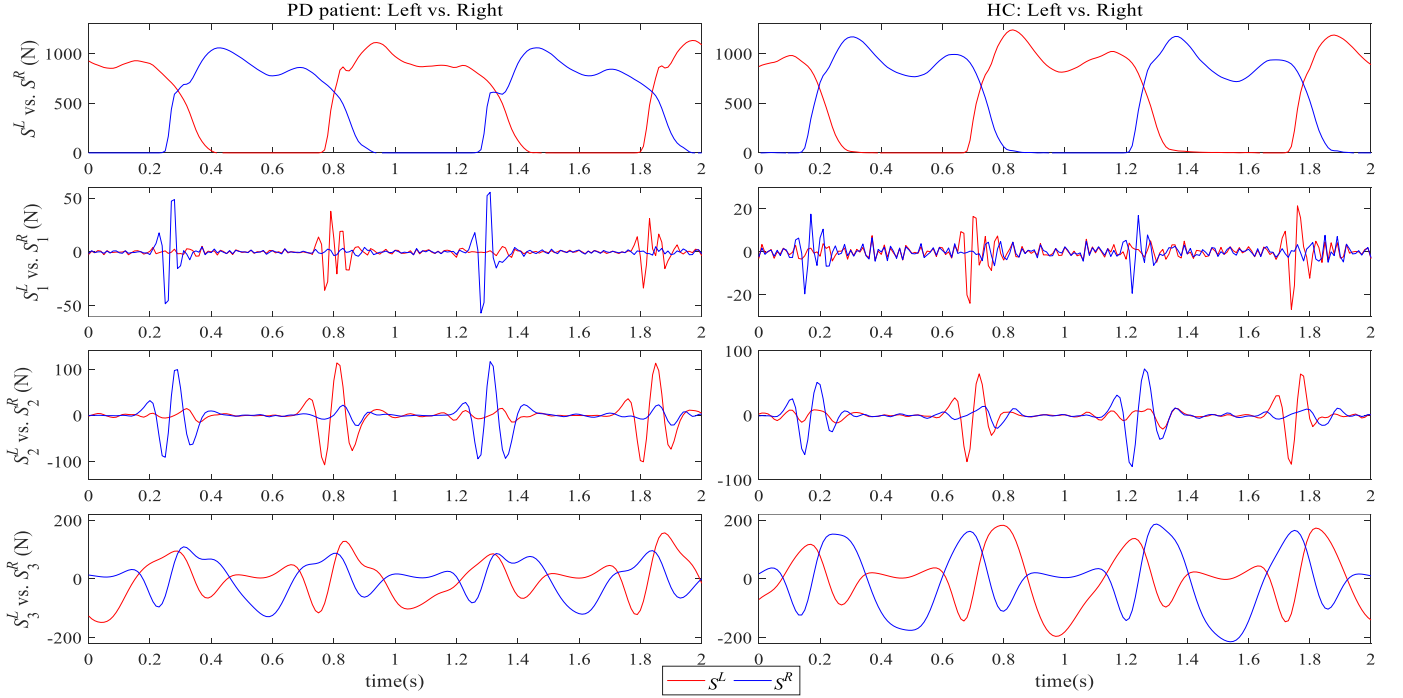
Fig. 1. EEMD analysis of the VGRF signals obtained from one HC individual and one PD patient. The VGRF signals of the left and right foot are represented in red and blue respectively. The plots are as follows, from top to bottom: the original VGRF signal, the first IMF, the second IMF, and the third IMF.

pairwise IMFs derived from both VGRF signals is calculated, which was expressed as:

$$\Delta\varphi_j^{LR}(t) = \varphi_j^R(t) - \varphi_j^L(t) \quad (j = 1, \ldots, J) \quad (10)$$

where $\varphi_j^L(t)$ and $\varphi_j^R(t)$ represent the instantaneous phases of the jth IMF derived from the VGRF signals of the left and right foot respectively. $\Delta\varphi_j^{LR}(t)$ indicates their phase difference.

If there is a high degree of consistency between these two IMFs, their phase difference will be almost constant over time; otherwise their phase difference will fluctuate dramatically over time [12]. The instantaneous phase coherence (*Coh*) measurement between S_j^L and S_j^R can then be calculated as:

$$Coh(S_j^L, S_j^R) = \frac{1}{T}\left|\int_0^T e^{i\Delta\varphi_j^{LR}(t)}dt\right| \quad (j = 1, \ldots, J) \quad (11)$$

where $e^{i\Delta\varphi_j^{LR}(t)}$ is a vector with unit length on a complex plane. T is the length of the signal. S_j^L and S_j^R represent the jth IMF decomposed from the left and right foot respectively. If the *Coh* coefficient is close to 1, it means that the instantaneous phase difference changes only slightly over time, which indicates that there is a strong correlation between IMF pairs. If the *Coh* coefficient is close to 0, we can infer that the instantaneous phase difference of the paired IMFs changes markedly over the entire time period [12].

b) Causal Interaction Strength Evaluation: Causal inference between pairwise IMFs derived from both VGRF signals is based on Galilei's principle: cause is that which, when present, is followed on by effect; when removed, the effect is removed [11]. Specifically, there are three key steps to achieve estimation of CIS [12]:

Step 1: Decompose both VGRF signals (S^L and S^R) into two sets of IMFs (S_j^L and S_j^R) and determine the instantaneous phase coherence between each pairwise IMFs;

Step 2: Remove the qth IMF in a given VGRF signal (e.g., S^L), and then produce a new VGRF signal through the removal of the qth IMF (e.g., $S^{L(-q)}$). Then perform a redecomposition procedure to generate a new set of IMFs (e.g., $S_j^{L(-q)}$) and recalculate the instantaneous phase coherence between the original IMFs in one VGRF signal (e.g., S_j^R) and the re-decomposed IMFs in the other VGRF signal (e.g., $S_j^{L(-q)}$);

Step 3: Because each IMF represents a dynamic process operating on different time scales, we regard the phase coherence between the paired IMFs as coordinates in a multidimensional space. Thus, the CIS can be quantified by the variance-weighted Euclidean distance between the phase coherence of the paired IMFs decomposed from the original signals (S_j^L vs. S_j^R) and the phase coherence of the paired original IMF and re-decomposed IMF (e.g. $S_j^{L(-q)}$ vs. S_j^R). The formula for the CISes between the qth IMF decomposed from S^L and S^R can be calculated as follows:

$$D(S_q^L \to S_q^R) = \left\{\sum_{j=1}^J W_j[Coh(S_j^L, S_j^R) - Coh(S_j^{L(-q)}, S_j^R)]^2\right\}^{\frac{1}{2}} \quad (12)$$

$$D(S_q^R \to S_q^L) = \left\{\sum_{j=1}^J W_j[Coh(S_j^L, S_j^R) - Coh(S_j^L, S_j^{R(-q)})]^2\right\}^{\frac{1}{2}} \quad (13)$$
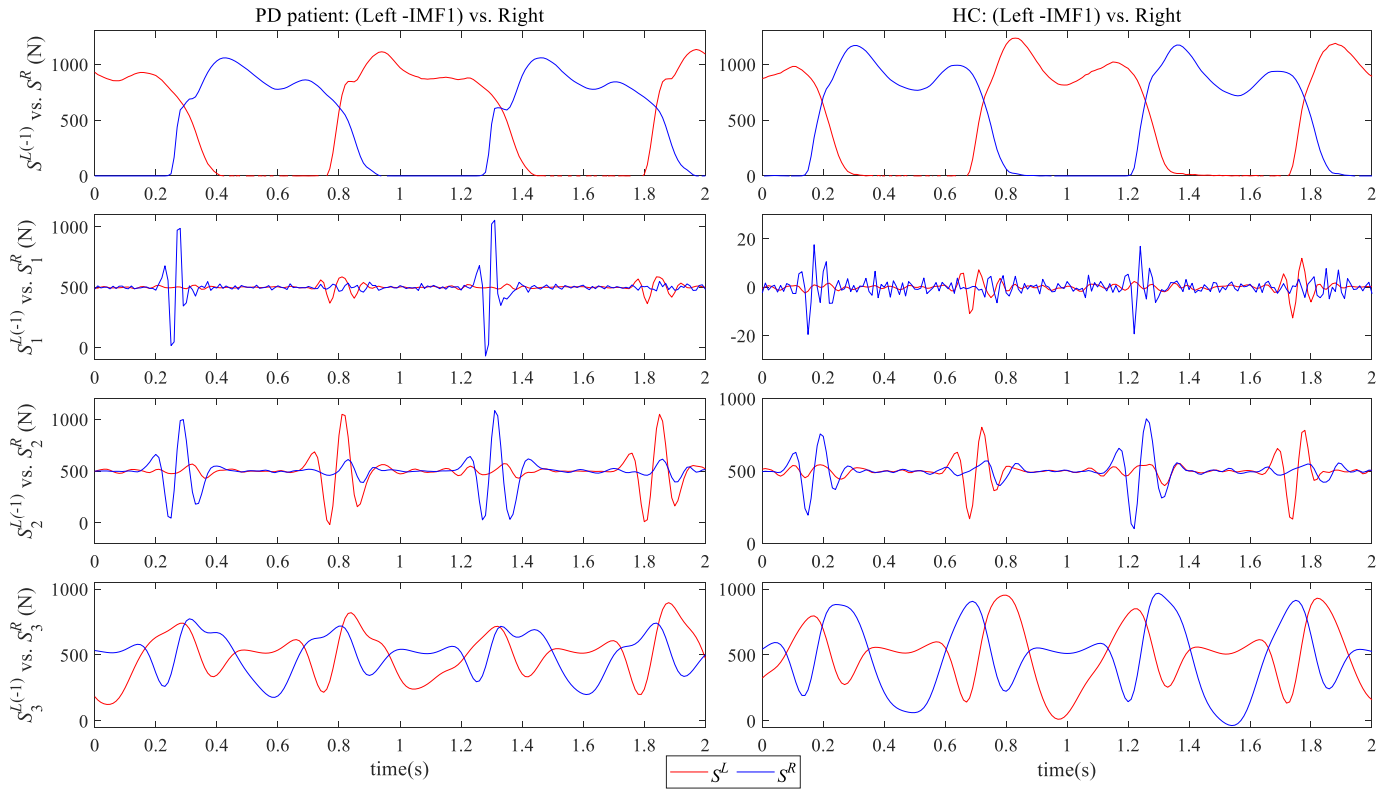
Fig. 2.   The re-decomposed IMFs of $S^{L(-1)}$ and the original IMFs of S^R of one PD patient and one HC individual based on the EEMD analysis. $S^{L(-1)}$ is obtained by subtracting the first IMF from S^L. According to Fig. 1 and 2, the CIS estimation for $D(S_1^L \rightarrow S_1^R)$ can be achieved.

$$W_j = (Var_j^L \times Var_j^R) / \sum_{j=1}^{J} (Var_j^L \times Var_j^R) \tag{14}$$

where coefficient $D(S_q^L \rightarrow S_q^R)$ represents the causal effect of the qth IMF in S^L on its corresponding IMF in S^R. $S_j^{L(-q)}$ represents a new set of IMFs, which have been re-decomposed from VGRF signal S^L with the removal of its qth IMF. Coefficient $D(S_q^R \rightarrow S_q^L)$ represents the causal effect of the qth IMF in S^R on its corresponding IMF in S^L. $S_j^{R(-q)}$ represents a new set of IMFs, which are re-decomposed from VGRF signal S^R with the removal of its qth IMF. W_j indicates the weight based on the variance of the jth IMF decomposed from S^L and S^R, namely Var_j^L and Var_j^R. Fig. 2 shows the original IMFs of S^R and the re-decomposed IMFs of $S^{L(-1)}$ for one PD patient and one HC individual based on the EEMD analysis. $S^{L(-1)}$ is obtained by subtracting the first IMF from S^L. According to Fig. 1 and 2, the CIS estimation for $D(S_1^L \rightarrow S_1^R)$ can be obtained. Fig. 3 shows the original IMFs of S^L and the re-decomposed IMFs of $S^{R(-1)}$ for one PD patient and one HC individual based on the EEMD analysis. $S^{R(-1)}$ is obtained by subtracting the first IMF from S^R. According to Fig. 1 and 3, the CIS estimation for $D(S_1^R \rightarrow S_1^L)$ can be obtained.

It should be noted that the motor symptoms of PD patients are often asymmetric, since their abnormal gait usually occurs first on one side and then on the other, and the onset side has different clinical manifestations compared to the other side [18]. However, this data set does not provide any information about which lower limb of a given PD patient has the initial motor dysfunction. Thus, CISes in different directions,

that $D(S_q^L \rightarrow S_q^R)$ and $D(S_q^R \rightarrow S_q^L)$, were averaged, denoted as $\overline{D_q}$.

C. Statistical Analysis

In this study, in order to evaluate whether PD significantly alters the causality of both feet during walking, statistical test was performed. Due to the non-normal distribution of $\overline{D_q}$ (detected by Jarque-Bera test at 5% significance level), the nonparametric statistical analyses were employed in this study. In addition, considering the potentially overpowered results caused by the size of the dataset [19], we adopted the bootstrap method. The specific procedures for statistical analysis are as follows.

In the first section, we examined the difference of $\overline{D_q}$ between PD patients and HC individuals through bootstrap-based Wilcoxon rank-sum tests. Specifically, sample size was initially determined for bootstrap, and the calculated appropriate sample size was 11 (The R package named "samplesize" was used to perform sample size calculation [20]. In this software package, the power was set to 0.9 and the significance level was set to 0.05). Then, 11 subjects were randomly selected from 93 PD patients and 73 HC individuals, respectively. In comparing the two subsets, Wilcoxon rank-sum test was used, and the corresponding p-value was obtained. These operations were repeated 1000 times and 1000 p-values were gained. To control the false discovery rate, these p-values were subsequently fused by harmonic mean p-value (HMP) technique [21]. It should be noted that, for HMP, the critical value of significance depends on the false positive rate α and the number of tests [21], which were set to 0.05 and 1000 in
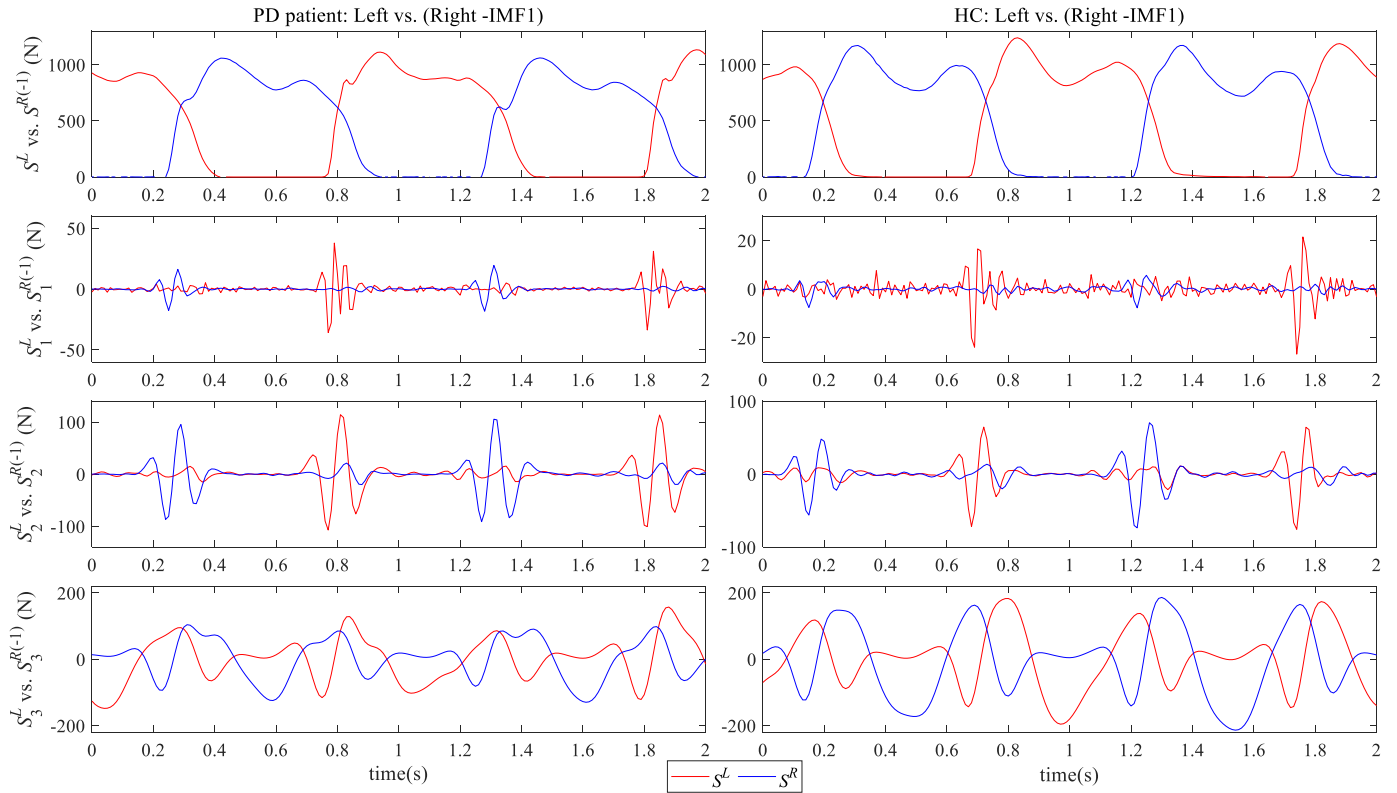
Fig. 3. The original IMFs of S^L and the re-decomposed IMFs of $S^{R(-1)}$ for one PD patient and one HC based on the EEMD analysis. $S^{R(-1)}$ is obtained by subtracting the first IMF from S^R. According to Fig. 1 and 3, the CIS estimation for $D(S_1^R \rightarrow S_1^L)$ can be obtained.

this study, respectively. According to [21], the calculated critical value of significance for HMP should be 0.034.

In the second section, the correlation coefficients between $\overline{D_q}$ and the PD progression scores (i.e. HY score and TUG score) were evaluated through bootstrap-based Spearman correlation test. Concretely, the sample size for bootstrap was initially calculated using the R package named "pwr" [22] (In that package, correlation coefficient was set at 0.8; the power was set to 0.9; and the significance level was set at 0.05), and the sample size for this study was 12. Next, Spearman correlation test was performed on the features and PD progression scores of 12 randomly selected subjects, which yielded one correlation coefficient and one p-value. These operations were repeated 1000 times, and thus 1000 correlation coefficients and 1000 p-values were obtained. Finally, these p-values were fused by HMP technique (the critical value of significance for HMP is also 0.034), and the arithmetic mean, as well as 95% confidence interval of 1000 correlation coefficients, were calculated.

D. Classification

In order to further estimate the effectiveness of our proposed approach for disease detection, the calculated $\overline{D_q}$ values were used for two-group classification. Similarly, to avoid the potential overpowered result, we performed classification on bootstrap subsamples [23]. And five commonly used classifier models, namely logistic, multilayer perceptron (MLP), decision tree (DT), support vector machine (SVM), k-nearest neighbor (KNN) were selected. Concretely, for each feature and classifier model, we first divided the feature

dataset randomly into 10 folds for cross-validation (i.e., one-fold for validating and remaining nine folds for training). Then, we randomly selected 1000 subsets from these nine folded training datasets and built 1000 classifiers on them respectively. Finally, the remaining one-fold dataset used for validation was successively fed into the 1000 trained classifiers. Thus, 1000 groups of classification results were obtained. For each validating sample, the label predicted by the majority of the classifiers was regarded as its final classification result. This procedure was repeated until each of the 10 folds had served as the validation set. And the mean of area under the receiver operating characteristics curve (AUC) values of the repeats, was taken as the performance index of that feature.

E. Method Comparison

To assess the practicability of our proposed method, the approaches mentioned in the introduction part were compared, including causal index, symmetry index, cross-correlation, and discrete wavelet transform (DWT). In order to analyze the gait in three frequency bands as our method does, VGRF signals were initially separated by Butterworth filters. According to previous research, EEMD can be interpreted as a filter bank of overlapping band-pass filters [24], thus, the frequency bands of Butterworth filters were set to the ranges of 13Hz-25Hz, 6Hz-13Hz and 0-6Hz to approximate the frequency distribution of the extracted IMFs. Then, the four methods mentioned above were applied to the high, intermediate and low frequency components of VGRF signals, respectively. In the first three methods, one feature was extracted from each frequency component, while in the method
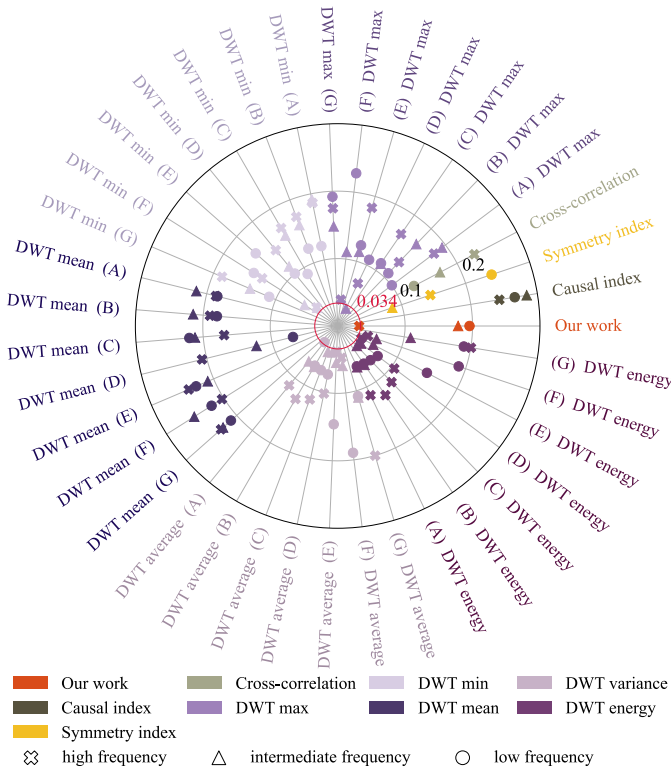
Fig. 4. Fused *p*-values of bootstrap-based Wilcoxon rank-sum tests for PD patients and HC. The letters A to G indicate the features derived from the six detail coefficients (from level 1 to 6) and one approximation coefficient of VGRF signals after DWT in sequence. The red circle represents the critical value of significance 0.034 (false positive rate $\alpha = 0.05$, number of tests = 1000).

Fig. 5. The results for bootstrap-based Spearman correlation analysis between HY score and the features of all methods. The bar indicates 95% confidence interval. The letters A to G represent the features derived from the six detail coefficients (from level 1 to 6) and one approximation coefficient of VGRF signals after DWT in sequence. The asterisk indicates that the HMP is less than critical value of significance 0.034 (false positive rate $\alpha = 0.05$, number of tests = 1000).

based on DWT, 35 features were extracted from each frequency component, including the maximum, minimum, mean, variance and energy of six detail wavelet coefficients (from level 1 to level 6) and one approximate coefficient. Finally, the above extracted features were used for statistical analysis and classification, to serve as a benchmark for the comparison of our proposed method.

III. RESULTS

Fig. 4 shows the fused *p*-values of the Wilcoxon rank sum tests for our proposed and comparative methods. It is apparent that only three features can significantly distinguish the two groups, that is, $\overline{D_1}$ and the DWT-based features extracted from intermediate and low frequency band of VGRF signals. It should be noted that, the average values of $\overline{D_1}$ in the PD patients and HC individuals are 0.115 and 0.075, respectively. This suggests that in the high frequency band, PD patients have stronger bilateral causal reaction compared to HC individuals.

Fig. 5 shows the results of Spearman correlation test between HY score and the features extracted by all methods. Obviously, only $\overline{D_1}$ and the DWT-based features from the intermediate and low frequency bands of VGRF signals can reveal the progression of PD patients. It should be noted that $\overline{D_1}$ has the highest absolute value of correlation coefficient among all the features as mentioned above. Fig. 6 shows the results of Spearman correlation test between TUG score and the features extracted by all methods, which are similar with the results shown in Fig. 5.
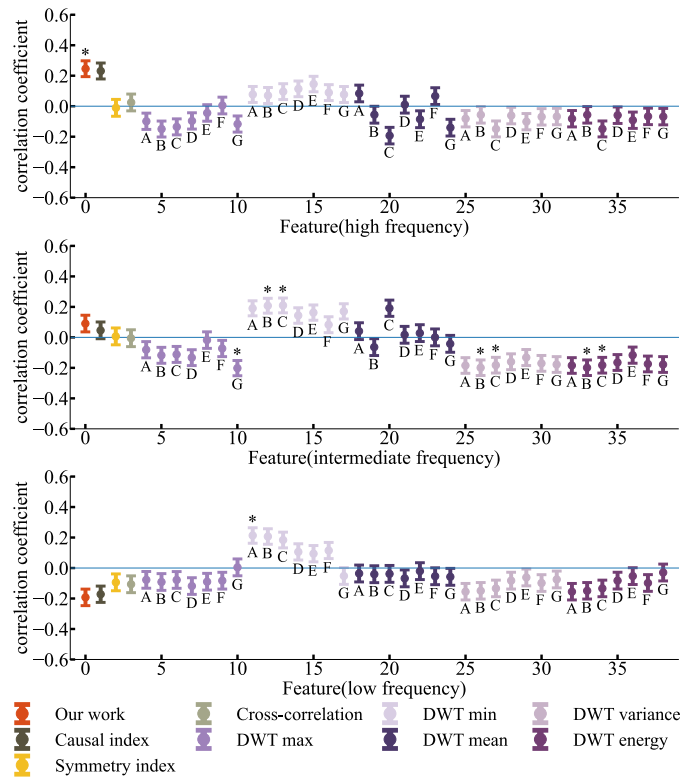
Fig. 7 shows the AUC values for the classification of PD and HC. $\overline{D_1}$ achieved higher AUC values compared with other features extracted by different methods from various frequency bands.

IV. DISCUSSION

The understanding of human gait has, for a long time, involved researchers from numerous different scientific disciplines such as biomechanics, functional anatomy, physiology, and neuroscience. Presently, an increasing number of data scientists are also participating in this field, and one of the purposes of their research is to provide new perspectives for the analysis of walking data, which might reveal biological mechanisms that traditional methods cannot obtain [9], [10].

Causal relationship exists widely in various physiological systems, such as cardiovascular system, nervous system and so on. In addition, many new physiological mechanisms have been discovered through causal analysis. Therefore, causal analysis in medicine has become a research hot spot in recent years. For cardiovascular system, Faes *et al.* found that systolic blood pressure may causally influence changes in cardiac cycle [25]. For neural system, it has been recognized for a long time that the interaction between brain neurons is directional, that is, there exists causality among them [26]. The ability of assessing the causal relationship between brain regions is not only important for exploring brain mechanisms, but it can also provide ideas for the diagnosis and treatment of epilepsy, Alzheimer's disease and other brain diseases.
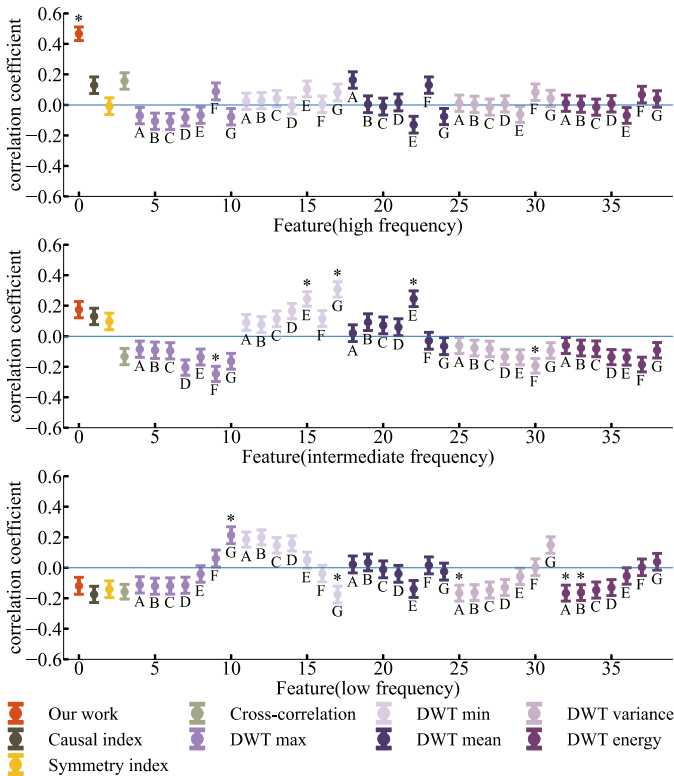
Fig. 6. The results for bootstrap-based Spearman correlation analysis between TUG score and the features of all methods. The bar indicates 95% confidence interval. The letters A to G denote the features derived from the six detail coefficients (from level 1 to 6) and one approximation coefficient of VGRF signals after DWT in sequence. The asterisk indicates that the HMP is less than the critical value of significance 0.034 (false positive rate $\alpha = 0.05$, number of tests = 1000).
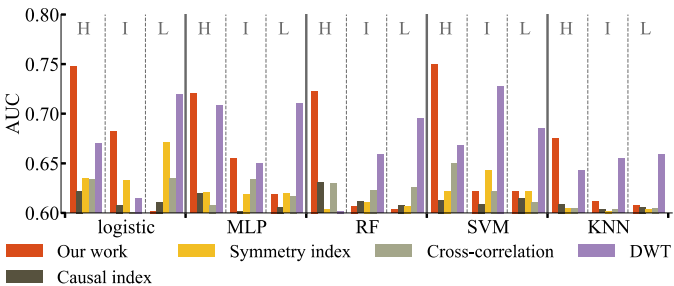
Fig. 7. AUC values for the classification of PD patients and HC. The letters H, I and L indicate the features extracted from high, intermediate, and low frequency bands of VGRF signals, respectively.

Furthermore, in recent years, many papers have pointed out that causality exists not only within a single physiological system, but also among different physiological systems. For example, Porta *et al.* found that strong causality exists between cardiovascular system and nervous system, which constantly affect each other [27].

Gait is a type of motion accomplished by the cooperative movement of bilateral lower limbs. It is obvious that there must be a causal relationship between the two lower limbs for the following reasons: (1) In terms of gait, we can imagine that if one side of the lower limb is completely unaffected by the other, the walking pattern with one foot removed, should be exactly the same as the walking pattern with two feet. In other words, if one side of the lower extremity is completely unaffected by the other, the kinetic/kinematical signals recorded during walking with one foot removed will be exactly the same as those recorded during walking with two feet. However, that is obviously not going to happen. Therefore, it is reasonable to infer that the bilateral lower limbs constantly affect each other during walking. (2) A number of previous studies have implied that the lower limbs are constantly causally influencing each other during walking. For example, Artemiadis *et al.* applied vertical perturbations on the unilateral leg of the subject walking on the split-belt treadmill and found out that when one leg looses the walking surface, the contralateral leg was observed to try to land earlier [28]. Dietz *et al.* changed unilateral belt speed with a constant contralateral speed to observe the reflection of the subjects while they walked on the split-belt treadmill. They discovered that the space-temporal behavior of one leg varied with the speed of the other [29]. Kuo *et al.* studied the dynamic walking model and found out that the foot placement of the swing leg must make lateral adjustments constantly to achieve bilateral stabilization [30]. (3) In addition to the study of HC individuals, similar phenomena have been observed in clinical practice. Boonstra *et al.* perturbed the PD patients with two independent continuous multi-sine perturbations, and they reported that PD patients compensate for balance control asymmetries by increasing the relative contribution of the leg of their least affected body side [31]. Karnath *et al.* reported that for patients with hemiplegia, the center of gravity of their body will tilt to the side of hemiplegia when they walk, but the side that is not affected, as compensation, will show abduction and extension to help in the push toward the affected (paretic) side [32]. Echeverria *et al.* conducted a research and observed that for patients with leg length discrepancy, whose paired lower extremity limbs have a noticeably unequal length, there are also compensation strategies between their lower limbs, including calcaneal eversion, toe walking, circumduction, hip flexion and knee flexion [33]. These patients express decreased stance time and stride length in the shorter leg, which may indicate that the shorter leg changes its movement pattern to adapt to the movement pattern of the longer one. Sousa *et al.* observed the subjects with stroke during step-to-step transition of walking and discovered that the lower performance of one limb in forward propulsion during gait is not only related to ipsilesional supraspinal damage but also to a dysfunctional influence of the contralateral limb [34]. Therefore, through clinical observations, it is easy to realize that when one side of a person is disturbed by the disease, the movement mode of the other side will also change. In other words, in the process of walking, the two sides of the individual causally influence each other, rather than being independent.

Thus far, no study has focused on the causal relationship analysis involved in gait except a recent paper published by Gong *et al.* [4]. As mentioned in the introduction, our article has made the following two improvements: (1) The simultaneous nature of causal interaction of both legs are included in the analysis of this study. Simultaneous causation means that the cause has already had an effect on the outcome at the moment the cause occurs [7]. The succession of the time of the cause and effect is produced because the cause cannot achieve the totality of its effect in one moment [12]. In fact,

this phenomenon has been widely discovered in different physiological systems, such as cardiovascular regulation and cerebrovascular regulation [5]. In the field of kinesiology, it is generally believed that an individual's current state of motion is the result of instantaneous interaction between various parts of the body. Of course, the same rule applies for walking [35]. With regard to gait analysis, it is well-known that a gait cycle consists of two periods of single support (when one leg is on the ground and the other leg is in the air) and two short periods of dual support (when both legs are on the ground) [35]. As can be seen, the criterion of gait stage classification also depends on the relationship of instantaneous movement between the two legs. More importantly, many studies have shown that causal inference is not very accurate if instantaneous causality is not considered (when the immediate lag is equal to zero) [5]–[7]. Thus, due to the facts mentioned above, the simultaneous causal interaction between bilateral gait was taken into account for purposes of analysis in this study. (2) As is widely known, time series observed in nature usually contain oscillatory components within a specific frequency band [36], [37]. For physiological signals, such as electroencephalography, their oscillatory components are able to reflect individuals' different physiological mechanisms, and the causal network they construct can even be employed for purposes of disease diagnosis [36], [37]. With regard to kinetic (and kinematic) signals, recent studies have found that they are also composed of oscillatory components with different levels of physiological significance [9], [10]. However, the causal interaction between both feet have not been investigated yet. Therefore, in this study we took the VGRF signals of PD patients and HC individuals as an example, and conjectured that PD might change the frequency-specific causal interactions of VGRF signals recorded while walking.

In this study, the VGRF signals with 100 Hz sampling rate was used to perform gait analysis. Previous studies have pointed out that through the analysis of GRF signals recorded at 960 Hz sampling rate, the highest frequency of the GRF signals was 24.37 Hz when the subjects walked at comfortable speed [38]. Therefore, the sampling rate of 100 Hz is basically enough to capture the frequency domain information of VGRF signals. In addition, many literature have used the data with 100 Hz or less sampling rate to analyze gait [38]–[40].

As the first step of causal decomposition, the EEMD method was implemented to extract the intrinsic oscillatory components embedded in VGRF signals. According to previous studies, EEMD has many advantages: (1) Compared with wavelet decomposition and Fourier transform, EEMD is a type of self-adaptive and data-driven approach that does not require setting any basis function in advance. Thus, EEMD is able to separate signals into IMFs, each of which can be generally associated to a physical aspect of the process from which the signal is obtained [9]. (2) EEMD can be regarded as a substantial improvement over empirical mode decomposition (EMD). The primary drawback of EMD is the mode mixing caused by the interference of random noise on the original signal, which cannot be completely removed by filter. Mode mixing means that there is a serious frequency distribution overlap between different IMF components, which makes these IMFs fail to meet the requirements of orthogonality and

separability. EEMD is a noise-aided data analysis method, and its main approach is to eliminate the random noise that affects the original signal by using the zero-mean characteristics of white noise [15]. (3) Kinetic and kinematic signals are non-linear and non-stationary. In this case, the frequency of the wave changes with time, and its profile is no longer a simple sine or cosine function. Thus, "harmonic distortions" will appear when Fourier transform is performed on it. These distortions show as sharpened crests and rounded-off troughs of wave forms, and the degree of distortion depends on the severity of nonlinearity [16]. Therefore, a predetermined basis (or a traditionally used basis, such as sine) may not be appropriate for the analysis of kinetic and kinematic signals. However, for EEMD, the local adaptive method, the amplitude and frequency of IMFs extracted by EEMD can vary over time, so the nonlinear and non-stationary signals can be effectively described [16]. Furthermore, many literatures have already proven that EEMD can effectively represent the physical nature of nonlinear and non-stationary data [15]. In other words, traditional band-pass filter based on frequency spectrum calculated by Fourier transforms may not be an effective tool to represent frequency-domain information [16]. Accordingly, the method of EEMD was employed in this paper, and this has been demonstrated to bypass assumptions of non-linear and non-stationary behavior, this resulted in a more precise instantaneous phase estimation for oscillatory components [12]. (4) In addition, the IMF extracted by EEMD was suitable for the Hilbert transform which was applied subsequently. Previous studies have shown that when the Hilbert transform is applied directly to nonlinear and non-stationary signals that have undergone traditional high-pass filtering (bandpass filtering /low-pass filtering), non-physical frequency negative values occur [16]. Hilbert transform can only be applied to narrow bandwidth signals, and IMF satisfies this requirement.

After decomposing the signal by EEMD, the Hilbert transform was used to calculate the instantaneous phase of each IMF and determine the phase coherence between the pairwise IMFs extracted from the left and right foot's VGRF signals. If a pair of IMFs are highly coherent, then their instantaneous phase difference is constant; otherwise, it fluctuates considerably over time. In the study of biomedical signals, a problem of particular interest is finding the dependency between the two signals. The most straightforward method is the application of cross measures, either cross-correlation or coherence. Cross-correlation operates in the time domain and coherence in the frequency domain. For time series mainly characterized by cycles and rhythms such as VGRF signals, coherence is usually the preferred choice. In addition, phase coherence allows the instantaneous phase dependency to be calculated without being subjected to the effect of time lag between cause and effect (i.e., the time precedence principle), thus avoiding the constraints of time lag in predictive causality methods [12]. Compared to conventional methods, it has been proved that causality measurement based on phase coherence can offer a more robust and reliable causality performance [12]. Up to now, many previous researches have used phase coherence to measure the relationship between two physiological signals [17], which also proved the validity of phase coherence.

According to the calculated phase coherence, the CISes between bilateral pairwise IMFs were estimated, and then averaged as $\overline{D_q}$ due to the potential causal asymmetry. The reasons are as follows: (1) According to previous studies, healthy adults can fine-tune their movement without attention, this is called motor automaticity [41]. But for PD patients, the connectivity from the anterior putamen to the primary motor cortex is decreased, and the dopamine in their posterior putamen is significantly depleted [42]. Therefore, they appear to lose previously stored automatic skills, and, simultaneously, have difficulty in recovering them or acquiring new ones [42]. In addition, putamen exists in the bilateral hemispheres of the brain. They separately control the body's unilateral motor automaticity and exhibit almost the same performance in a healthy condition. But for PD patients, bilateral putamen commonly has dopaminergic depletion in varying degrees [43]. Under these conditions, bilateral motor automaticity degenerates and their severity may be inconsistent. One side may not be able to fine-tune its motion as much as the other side and needs more compensation from contralateral motion regulation, which may indicate that one side have a greater causal effect on the other side. (2) Due to the brain's contralateral control mechanism, the unilateral substantia nigra is mostly associated with the contralateral movement of the body. In a healthy condition, they function almost as well as each other. However, for PD patients, progressive degeneration of the substantia nigra occurs with greater neuronal loss in one side [44]. Under these circumstances, the function of bilateral substantia nigra is impaired in different levels. And the different severity of motor symptoms, include bradykinesia, rigidity, and tremor, appear on both sides of the body [44]. To maintain the movement, one side may compensate the contralateral more, which may indicate causal asymmetry.

In order to evaluate whether PD significantly alters the causality of both feet during walking, statistical analyses were performed. Since excessively large samples may make the results overpowered, the bootstrap-based statistical analysis was implemented in this study. To control the false discovery rate, HMP, the widely used technique, was performed, and its advantages are as follows: (1) Combining p-values is one of the most commonly used statistical strategy to synthesize information from multiple tests. So far, many p-value fusion methods have been proposed, including Fisher's method, Brown's method, Kost's method, *et al* [45]. HMP, as one of them, combines the p-values together, which makes it convenient to compare with the critical value of significance to judge whether the null hypothesis of the statistical test should be rejected. (2) Previous p-value combination techniques like Fisher's method makes the strong assumption that tests are independent, but HMP is robust to dependency between p-values and thereby avoids the restrictive assumption [21]. Thus, it applies not only to independent conditions but also non-independent conditions. Since the subsets extracted by bootstrap method are not completely independent of each other, it is more accurate to use HMP to fuse the p-values obtained from each subset. (3) HMP is insensitive to the number of tests. Unlike traditional methods such as Bonferroni correction, that require the critical value of significance to decrease linearly with the increase in the number of tests, HMP only requires the critical value of significance to decrease logarithmically as the number of tests increases [21], which prevents the critical value from being too stringent when the number of tests is large. (4) HMP enables adaptive multiple testing correction [21]. This means that, when there are numerous p-values that are far below the critical value, smaller fused p-values will be produced. On the contrary, when there are few significant p-values, HMP technique tends to be conservative and strict. In the extreme case where one p-value is much more significant than others, the HMP technique becomes equivalent to Bonferroni correction. (5) So far, a large number of studies have used HMP to combine the p-values, including but not limited to combining the p-values extracted from bootstrap analysis [46]–[50]. Such widespread use of HMP also proves its effectiveness. Therefore, in this study, the fused p-value was taken as the result of p-values extracted from the statistical analysis performed by bootstrap.

As shown in Fig. 5 and Fig. 6, for causal decomposition, only the feature for high frequency, can significantly distinguish two groups and exhibit the significant correlation with PD progression. According to previous literature, the high frequency band of VGRF signals can reflect the walking performance of individuals when their foot just touches the ground (heel strike) or leaves the ground (toe-off) (see the IMF1 shown in Fig. 1) [9], [51]. These time periods usually require the participation of complex postural controls, such as postural adjustment anticipation and external environment adaptation, to maintain balance [35]. Therefore, these controls and periods are also considered to be the key for walking effectively, efficiently, and smoothly. However, motor dysfunctions such as postural instability and stiffness of the lower limbs makes it easy for PD patients to lose their balance, especially during these two time periods. In order to prevent falls, PD patients will consciously or unconsciously increase the degree of coordination between their lower extremities. In addition, this inference is also supported by a large number of literatures, which have shown that in many gait stages, PD patients mainly have a great difference in heel strike when compared to HC individuals. Specifically, their heel strike patterns change from the normal 'heel-toe' gait to the abnormal 'toe-heel' gait or a gait with forefoot strike only [41]. This is mainly due to their walking postural changes, such as thoracic kyphosis, hip and shoulder abduction, knee and elbow flexion [52]. Apart from these, the body of PD patients is in an unstable position during walking, when the heel of one leg strikes the ground and the toes of the other leg are still in contact with the floor [35]. Therefore, PD patients try to avoid this unstable posture, which requires more coordination of the feet, and this can be seen as an adaptive mechanism to compensate for instability.

Apart from this, we also observed a positive increase in feature $\overline{D_1}$ as the disease progresses in Fig. 5 and Fig. 6, this indicates that with the development of disease, PD patients need increased coordination between legs when heel strikes. From here we see that it is very necessary to analyze the CISes of VGRF signals at different frequency bands. Although the correlation coefficients did not seem very high, we found that the confidence intervals of the correlation coefficients did

not contain 0, indicating that there was indeed a correlation between the features we extracted and disease severity. The scatter plot of the correlation coefficient between the feature $\overline{D_1}$ and the scale score are shown in the supplementary material.

The low correlation coefficient between our extracted features and the scale score might be as a result of the following reasons: (1) According to previous literature, the clinical manifestations of PD vary widely because they span across motor and non-motor related symptoms [53], [54]. The range of initial motor symptoms include tremor (70.5%), rigidity and bradykinesia (19.7%), akinesia (12.6%), gait disorder (11.5%), myalgia and muscle spasm (8.2%), muscular weakness (2.7%), mask face (1.6%) etc. [53]. The percentages in parenthesis indicate the proportion of PD patients with these motor symptoms. On the other hand, the non-motor related symptoms comprise autonomic nervous dysfunction, neuropsychiatric problems (change in mood, cognition, behavior or thinking), sensation (especially changes in smell), difficulty in sleeping etc [54]. A large number of literatures have reported that for PD patients, either motor or non-motor related symptoms would be their main indicators, or it could also be accompanied by a severe simultaneous manifestation of these two groups of symptoms [54], [55]. Therefore, it is apparent that not all PD patients have gait disorder as their main symptom, and this could be the possible reason why our extracted features had no strong correlation with Hoehn & Yahr score (and TUG score). (2) As we all know, gait procedure involves the participation of a number of different physiological components, including the muscles, joints, cerebral cortex, cerebellum, spinal cord, and more. Presently, an increasing number of researches are based on multimodality. This is so, because a mode can only show one aspect of the motion characteristics. In this paper, only one mode, VGRF, is provided in the dataset and it may not be sufficient to fully express the motor characteristics of PD. Therefore, we suggest the extraction of different features of different modes in the future, and the use of multiple regression or ensemble learning methods to study the relationship between these characteristics and diseases.

In addition, inspired by [56], we calculated the relative power. we discovered that $\overline{D_1}$ exhibited significant difference between two-subject groups, and its corresponding IMF was with 1.9% relative power to the original VGRF signal. This may be due to the following reasons: (1) Such IMF reflects high frequency component of VGRF signals and corresponds to the heel strike stage. At this stage, the procedure of foot load response and weight acceptance is just beginning [57]. Therefore, compared with the amplitude of VGRF in all gait stages, its amplitude in this period is relatively small. (2) Heel strike describes the stage in gait at which the heel first makes contact with the walking surface, and this only lasts 2% of the entire gait cycle [57]. Thus, the duration for this period is relatively short. (3) Many previous studies have observed that 99% of the power of VGRF is mainly concentrated in the intermediate and low frequency band [14]. It can be seen that the motion characteristics of the heel strike stage is the main reason leading to the relatively low energy of the IMF with high frequency. However, this IMF is still very important.

As mentioned above, it does reflect the impact of PD on gait mechanism and bilateral causality, which cannot be reflected by other frequency components.

In order to evaluate the effectiveness of our work, the features extracted by the methods mentioned in introduction, were also used for statistical analysis and classification. Their results were taken as a benchmark for the comparison of our proposed method, and we achieved the best performance. It is worth noting that the purpose of this study is not to prove that our proposed approach is omnipotent for gait analysis, but to show that: (1) the study of bilateral gait causality in frequency domain has physiological significance; (2) diseases may lead to changes in gait causality, which has not been found in previous studies.

V. CONCLUSION

In summation, our study applied a new method for performing gait analysis, namely causal decomposition, which is based on analyzing the causal interaction of bilateral kinetic (or kinematic) signals at different frequency bands. Furthermore, this approach also considers the simultaneous nature of causal interaction for both feet during walking. To illustrate this approach, the VGRF signals of PD patients and HC individuals were used for analysis. The results show that PD only changes the causality of bilateral VGRF signals in the high frequency band, but not in other frequency bands. As can be seen, the identification of frequency-specific causal interactions is essential to understand the underlying mechanisms of walking and these mechanisms' relationship to PD. Finally, this approach may be used broadly in the fields of medicine and engineering, including the fields of neuroscience, sports science, rehabilitative medicine, and in the field of wearable devices.

REFERENCES

[1] D. Joshi, A. Khajuria, and P. Joshi, "An automatic non-invasive method for Parkinson's disease classification," *Comput. Methods Programs Biomed.*, vol. 145, pp. 135–145, Jul. 2017.

[2] A. Sant'Anna and N. Wickström, "A symbol-based approach to gait analysis from acceleration signals: Identification and detection of gait events and a new measure of gait symmetry," *IEEE Trans. Inf. Technol. Biomed.*, vol. 14, no. 5, pp. 1180–1187, Sep. 2010.

[3] D. Gouwanda and S. M. N. A. Senanayake, "Identifying gait asymmetry using gyroscopes—A cross-correlation and normalized symmetry index approach," *J. Biomech.*, vol. 44, no. 5, pp. 972–978, Mar. 2011.

[4] J. Gong, J. Lach, Y. Qi, and M. D. Goldman, "Causal analysis of inertial body sensors for enhancing gait assessment separability towards multiple sclerosis diagnosis," in *Proc. IEEE 12th Int. Conf. Wearable Implant. Body Sensor Netw. (BSN)*, Jun. 2015, pp. 1–6.

[5] L. Schiatti, G. Nollo, G. Rossato, and L. Faes, "Extended Granger causality: A new tool to identify the structure of physiological networks," *Physiol. Meas.*, vol. 36, no. 4, pp. 827–843, Mar. 2015.

[6] G. Deshpande, K. Sathian, and X. Hu, "Assessing and compensating for zero-lag correlation effects in time-lagged Granger causality analysis of fMRI," *IEEE Trans. Biomed. Eng.*, vol. 57, no. 6, pp. 1446–1456, Jun. 2010.

[7] I. Kant, E. Watkins, and W. Pluhar, *Critique of Pure Reason*. Cambridge, U.K.: Hackett Publishing, 1999.

[8] J. G. Nutt, B. R. Bloem, N. Giladi, M. Hallett, F. B. Horak, and A. Nieuwboer, "Freezing of gait: Moving forward on a mysterious clinical phenomenon," *Lancet Neurol.*, vol. 10, no. 8, pp. 734–744, Aug. 2011.

[9] R. Alkhatib, "Human locomotion analysis, classification and modeling of normal and pathological vertical ground reaction force signals in elderly," Ph.D. dissertation, Dept. Signal Image Process., Univ. Lyon, Lyon, France, 2016.

[10] B. L. Su, R. Song, L. Y. Guo, and C. W. Yen, "Characterizing gait asymmetry via frequency sub-band components of the ground reaction force," *Biomed. Signal Process. Control*, vol. 18, pp. 56–60, Apr. 2015.

[11] G. Galilei, *On Motion and On Mechanics*. Madison, WI, USA: Univ. of Wisconsin Press, 1960.

[12] A. C. Yang, C.-K. Peng, and N. E. Huang, "Causal decomposition in the mutual causation system," *Nature Commun.*, vol. 9, no. 1, pp. 1–10, Aug. 2018.

[13] A. L. Goldberger *et al.*, "PhysioBank, PhysioToolkit, and PhysioNet: Components of a new research resource for complex physiologic signals," *Circulation*, vol. 101, no. 23, pp. e215–e220, Jun. 2000.

[14] E. K. Antonsson and R. W. Mann, "The frequency content of gait," *J. Biomech.*, vol. 18, no. 1, pp. 39–47, Jan. 1985.

[15] Z. Wu and N. E. Huang, "Ensemble empirical mode decomposition: A noise-assisted data analysis method," *Adv. Adapt. Data Anal.*, vol. 1, no. 1, pp. 1–41, Jan. 2009.

[16] N. E. Huang *et al.*, "The empirical mode decomposition and the Hilbert spectrum for nonlinear and non-stationary time series analysis," *Proc. Roy. Soc. London. A, Math., Phys. Eng. Sci.*, vol. 454, no. 1971, pp. 903–995, Mar. 1998.

[17] F. Varela, J.-P. Lachaux, E. Rodriguez, and J. Martinerie, "The brainweb: Phase synchronization and large-scale integration," *Nature Rev. Neurosci.*, vol. 2, no. 4, pp. 229–239, Apr. 2001.

[18] A. van der Hoorn, H. Burger, K. L. Leenders, and B. M. de Jong, "Handedness correlates with the dominant parkinson side: A systematic review and meta-analysis," *Movement Disorders*, vol. 27, no. 2, pp. 206–210, Oct. 2011.

[19] S. F. Anderson, K. Kelley, and S. E. Maxwell, "Sample-size planning for more accurate statistical power: A method adjusting sample effect sizes for publication bias and uncertainty," *Psychol. Sci.*, vol. 28, no. 11, pp. 1547–1562, Nov. 2017.

[20] *Samplesize: Sample Size Calculation for Various t-Tests and Wilcoxon-Test*. Accessed: Dec. 24, 2016. [Online]. Available: https://cran.r-project.org/web/packages/samplesize/index.html

[21] D. J. Wilson, "The harmonic mean p-value for combining dependent tests," *Proc. Nat. Acad. Sci. USA*, vol. 116, no. 4, pp. 1195–1200, Jan. 2019.

[22] *PWR: Basic Functions for Power Analysis*. Accessed: Mar. 17, 2020. [Online]. Available: https://cran.r-project.org/web/packages/pwr/

[23] L. Breiman, "Bagging predictors," *Mach. Learn.*, vol. 24, no. 2, pp. 123–140, Aug. 1996.

[24] P. Flandrin, G. Rilling, and P. Goncalves, "Empirical mode decomposition as a filter bank," *IEEE Signal Process. Lett.*, vol. 11, no. 2, pp. 112–114, Feb. 2004.

[25] L. Faes, G. Nollo, and A. Porta, "Information domain approach to the investigation of cardio-vascular, cardio-pulmonary, and vasculo-pulmonary causal couplings," *Frontiers Physiol.*, vol. 2, p. 80, Nov. 2011.

[26] M. Kamiński, M. Ding, W. A. Truccolo, and S. L. Bressler, "Evaluating causal relations in neural systems: Granger causality, directed transfer function and statistical assessment of significance," *Biol. Cybern.*, vol. 85, no. 2, pp. 145–157, Aug. 2001.

[27] A. Porta, T. Bassani, V. Bari, G. D. Pinna, R. Maestri, and S. Guzzetti, "Accounting for respiration is necessary to reliably infer Granger causality from cardiovascular variability series," *IEEE Trans. Biomed. Eng.*, vol. 59, no. 3, pp. 832–841, Mar. 2012.

[28] P. K. Artemiadis and H. I. Krebs, "Interlimb coordination evoked by unilateral mechanical perturbation during body-weight supported gait," in *Proc. IEEE Int. Conf. Rehabil. Robot.*, Jun. 2011, pp. 1–5.

[29] V. Dietz, W. Zijlstra, and J. Duysens, "Human neuronal interlimb coordination during split-belt locomotion," *Exp. Brain Res.*, vol. 101, no. 3, pp. 513–520, Oct. 1994.

[30] A. D. Kuo and J. M. Donelan, "Dynamic principles of gait and their clinical implications," *Phys. Therapy*, vol. 90, no. 2, pp. 157–174, Feb. 2010.

[31] T. A. Boonstra, A. C. Schouten, J. P. P. van Vugt, B. R. Bloem, and H. van der Kooij, "Parkinson's disease patients compensate for balance control asymmetry," *J. Neurophysiol.*, vol. 112, no. 12, pp. 3227–3239, Dec. 2014.

[32] H. O. Karnath and D. Broetz, "Understanding and treating 'pusher syndrome,'" *Phys. Therapy*, vol. 83, no. 12, pp. 1119–1125, Dec. 2003.

[33] J. C. Echeverria, E. Rodriguez, A. Velasco, and J. Alvarez-Ramirez, "Limb dominance changes in walking evolution explored by asymmetric correlations in gait dynamics," *Phys. A, Stat. Mech. Appl.*, vol. 389, no. 8, pp. 1625–1634, Apr. 2010.

[34] A. S. P. Sousa, A. Silva, R. Santos, F. Sousa, and J. M. R. S. Tavares, "Interlimb coordination during the stance phase of gait in subjects with stroke," *Arch. Phys. Med. Rehabil.*, vol. 94, no. 12, pp. 2515–2522, Dec. 2013.

[35] A. Shumway-Cook and M. H. Woollacott, *Motor Control: Translating Research Into Clinical Practice*. Philadelphia, PA, USA: North American, 2016.

[36] S. Hamburg, R. Rosch, C. M. Startin, K. J. Friston, and A. Strydom, "Dynamic causal modeling of the relationship between cognition and theta–alpha oscillations in adults with down syndrome," *Cerebral Cortex*, vol. 29, no. 5, pp. 2279–2290, Mar. 2019.

[37] M. de Tommaso, S. Stramaglia, D. Marinazzo, G. Trotta, and M. Pellicoro, "Functional and effective connectivity in EEG alpha and beta bands during intermittent flash stimulation in migraine with and without aura," *Cephalalgia*, vol. 33, no. 11, pp. 938–947, Feb. 2013.

[38] N. Stergiou, G. Giakas, J. E. Byrne, and V. Pomeroy, "Frequency domain characteristics of ground reaction forces during walking of young and elderly females," *Clin. Biomech.*, vol. 17, no. 8, pp. 615–617, Oct. 2002.

[39] O. Afsar, U. Tirnakli, and N. Marwan, "Recurrence quantification analysis at work: Quasi-periodicity based interpretation of gait force profiles for patients with parkinson disease," *Sci. Rep.*, vol. 8, no. 1, pp. 1–12, Dec. 2018.

[40] A. H. Vrieling *et al.*, "Gait adjustments in obstacle crossing, gait initiation and gait termination after a recent lower limb amputation," *Clin. Rehabil.*, vol. 23, no. 7, pp. 659–671, Jul. 2009.

[41] M. Gilat *et al.*, "Dopamine depletion impairs gait automaticity by altering cortico-striatal and cerebellar processing in Parkinson's disease," *NeuroImage*, vol. 152, pp. 207–220, May 2017.

[42] T. Wu, M. Hallett, and P. Chan, "Motor automaticity in Parkinson's disease," *Neurobiol. Disease*, vol. 82, pp. 226–234, Oct. 2015.

[43] W. Lin, C.-T. Zuo, J.-J. Wu, L.-K. Yang, J. Zhu, and Y.-H. Wang, "Striatal asymmetry index and its correlation with the Hoehn & Yahr stage in Parkinson's disease," *Int. J. Neurosci.*, pp. 1–6, Sep. 2020.

[44] P. A. Kempster, W. R. Gibb, G. M. Stern, and A. J. Lees, "Asymmetry of substantia nigra neuronal loss in Parkinson's disease and its relevance to the mechanism of levodopa related motor fluctuations," *J. Neurol., Neurosurg. Psychiatry*, vol. 52, no. 1, pp. 72–76, Jan. 1989.

[45] W. Poole, D. L. Gibbs, I. Shmulevich, B. Bernard, and T. A. Knijnenburg, "Combining dependent P-values with an empirical adaptation of Brown's method," *Bioinformatics*, vol. 32, no. 17, pp. i430–i436, Sep. 2016.

[46] A. Graudenzi, D. Maspero, F. Angaroni, R. Piazza, and D. Ramazzotti, "Mutational signatures and heterogeneous host response revealed via large-scale characterization of SARS-CoV-2 genomic diversity," *iScience*, vol. 24, no. 2, Feb. 2021, Art. no. 102116.

[47] E. Whitman *et al.*, "A method for creating a burn severity atlas: An example from Alberta, Canada," *Int. J. Wildland Fire*, vol. 29, pp. 995–1008, Aug. 2020.

[48] S. Rodriguez *et al.*, "Machine learning identifies candidates for drug repurposing in Alzheimer's disease," *Nature Commun.*, vol. 12, no. 1, pp. 1–13, Feb. 2021.

[49] M. Alonge *et al.*, "Major impacts of widespread structural variation on gene expression and crop improvement in tomato," *Cell*, vol. 182, no. 1, pp. 145–161, Jul. 2020.

[50] N. E. Kogan *et al.*, "An early warning approach to monitor COVID-19 activity with multiple digital traces in near real time," *Sci. Adv.*, vol. 7, no. 10, Mar. 2021, Art. no. eabd6989.

[51] N. Strzalkowski, "Tactile perception across the human foot sole as examined by the firing characteristics of cutaneous afferents and mechanical properties of the skin," Ph.D. dissertation, Dept. Hum. Health Nutritional Sci. Neurosci., Univ. Guelph, Guelph, ON, Canada, 2015.

[52] A. Khlebtovsky *et al.*, "Progression of postural changes in Parkinson's disease: Quantitative assessment," *J. Neurol.*, vol. 264, no. 4, pp. 675–683, Feb. 2017.

[53] T. Friedmann, J. C. Dunlap, and S. F. Goodwin, *Advances in Genetics*, vol. 98. Cambridge, MA, USA: Academic, 2017.

[54] R. Erro *et al.*, "Clinical clusters and dopaminergic dysfunction in de-novo Parkinson disease," *Parkinsonism Rel. Disorders*, vol. 28, pp. 137–140, Jul. 2016.

[55] M. Lawton *et al.*, "Developing and validating Parkinson's disease subtypes and their motor and cognitive progression," *J. Neurol. Neurosurg. Psychiatry*, vol. 89, no. 12, pp. 1279–1287, Nov. 2018.

[56] D. A. T. Cummings *et al.*, "Travelling waves in the occurrence of dengue haemorrhagic fever in Thailand," *Nature*, vol. 427, no. 6972, pp. 344–347, Jan. 2004.

[57] N. Stergiou, *Biomechanics and Gait Analysis*. Cambridge, MA, USA: Academic, 2020, pp. 225–250.